J Therm Anal Calorim (2015) 120:1283–1291
DOI 10.1007/s10973-015-4448-9

The effect of urea and urea-modified halloysite on performance of PCL

Viera Khunová · Ivan Kelnar · János Kristóf · Jiří Dybal · Jaroslav Kratochvíl · Ludmila Kaprálková

Received: 21 October 2014 / Accepted: 14 January 2015 / Published online: 18 February 2015

Abstract The effects of urea and urea-modified halloysite nanotubes (HNT) on structure and properties of poly (ε-caprolactone) (PCL) were evaluated using mechanical testing combined with FTIR, DSC, DMA, and various microscopic techniques. The results indicate important changes in mechanical behavior by urea-mediated interchain hydrogen bonding in PCL, whereas no linking between PCL and HNT in the related nanocomposite was found. As a result, the improved mechanical behavior of nanocomposites with urea-modified HNT was caused by combination of the matrix modification and urea-aided enhanced dispersion of HNT. The additives do not have any marked effect on PCL crystallinity. HNT increases and urea reduces the overall rate of crystallization. Both additives show a moderate nucleating effect.

Keywords PCL · Urea · Halloysite · Nanocomposites · DSC

V. Khunová (✉)
Faculty of Chemical and Food Technology, The Slovak University of Technology, Radlinského 9, 812 37 Bratislava, Slovakia
e-mail: viera.khunova@stuba.sk

I. Kelnar · J. Dybal · J. Kratochvíl · L. Kaprálková
Institute of Macromolecular Chemistry, Academy of Sciences of the Czech Republic, Heyrovského nám. 2, 162 06 Prague, Czech Republic

J. Kristóf
Institute of Chemistry, University of Pannonia, P.O. Box 158, 8201 Veszprém, Hungary

Introduction

During the last two decades, a remarkable improving of end-use properties of polymers has been achieved by the incorporation of nanofillers. Numerous published papers were aimed at the modification of polymer matrices by nanofillers with various particle shape, size, and chemistry. In spite of the tremendous achievements obtained by application of carbon-based nanofillers, layered silicates are continually the most industrially attractive nanofillers for every type of polymer matrices, including the biodegradable ones.

The poly(ε-caprolactone) (PCL) belongs to the most important biodegradable polymers [1, 2]. However, there are several factors holding back the progressive development and applications of PCL. The main reason of limited PCL utilization is unsatisfactory mechanical properties, especially modulus and tensile strength. There was a great effort dedicated to improvement of mechanical properties of PCL by formation of blends [3–6] and composites [7, 8]. A very effective way to improve PCL mechanical properties is application of layered silicates [9–13]. Unlike traditional particulate fillers, such as calcium carbonate and kaoline, the improvement of mechanical properties is usually achieved at very low concentrations [14]. A further significant benefit of nanofillers application is increased biodegradability of PCL [11]. While most papers indicate that the improvement of end-use properties can be achieved by the application of layered silicates, it has recently been documented that tubular silicates, like halloysites, are useful, as well [15–17]. Dissimilarly to layered silicates, where intercalation (modification) is inevitable to achieve improvement of properties, there are examples in the literature documenting that no treatment of halloysite is necessary to attain acceptable filler dispersion and outstanding end-use properties [15–17]. A recent example of

outstanding improvement of PCL properties by using small amounts of untreated tubular halloysite (HNT) has been documented by Lee and Chang [17].

In our recent work on PP/HNT composites, it was found that modification of halloysite nanotubes by urea caused improved halloysite dispersion in nonpolar polypropylene matrix. However, due to poor interfacial interactions, no improvement of mechanical properties was observed. Surprisingly, improved mechanical properties were found when the reactive modifier, 4,4′-diphenylmethylenedimaleinimide (DBMI) was used to provide linkage between PP and HNT. The reaction between the DBMI ring and the OH group of HNT was supported by urea [18]. Dissimilarly to nonpolar polymer matrices, the application of urea and urea-modified halloysite can be advantageous in polar polymer systems. Based on the above, in the present work, we have focused on the investigation of possibilities of using urea-modified halloysite and urea itself in PCL.

Experimental

Materials

The poly(ε-caprolactone) (CAPA 6800, PCL, M_w = 80,000 g mol^{-1}, melting point = 60 °C, MFI = 2.4 g/10 min (2.16 kg, 160 °C) was obtained from Perstorp, Sweden. Halloysite was received from Biela Hora, Michalovce, Slovakia. Before modification, the halloysite was ground into powder using a laboratory ball mill. The powdered halloysite was purified and sieved. The average particle size of halloysite agglomerates was 10 μm (Fig. 1).

Halloysite intercalation by urea

The intercalation of urea into the halloysite was performed by mechanochemical means (dry grinding). A 10-g mixture of the clay and urea (mixed in 2:1 ratio) was produced using a Fritsch Pulverisette 5/2-type laboratory planetary mill. Milling was performed for 30 min in an 80 cm^3 capacity stainless steel bowl using 29 (110.3 g total) stainless steel balls (10 mm diameter each). The rotation speed was 374 rpm.

Composite preparation

The composites were prepared from poly(ε-caprolactone) and unmodified and/or intercalated halloysite (at 5 mass%) via melt mixing in a Brabender W50-E chamber at 140 °C using a rotor speed of 180 rpm with mixing time of 5 min. PCL containing 1 % urea was prepared in the same way.

Dog-bone-shaped specimens (a gauge length of 40 mm, EN ISO 527-2:2012, Sample size 5B) were prepared in a laboratory microinjection molding machine (DSM). The barrel and mold temperatures were 135 and 130 °C, respectively.

Mechanical testing

Tensile tests were carried out using an Instron 5800 apparatus at 22 °C and crosshead speed of 20 mm min^{-1}. At least eight specimens were tested for each sample. The Young's modulus (E), maximum stress (σ_m), and elongation at break (ε_b) were evaluated; the corresponding variation coefficients did not exceed 7, 2, and 15 %, respectively.

Dynamic mechanical thermal analysis (DMA) was performed in single-cantilever mode using a DMA DX04T apparatus at 1 Hz and heating rate of 1 °C min^{-1} from −120 to 100 °C.

Differential scanning calorimetry

DSC analysis was carried out using a Perkin-Elmer 8500 DSC apparatus. Cyclohexane and indium were used for

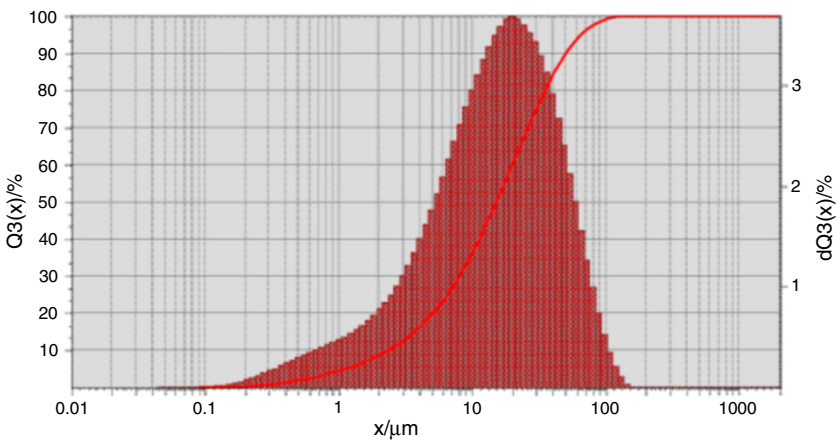

Fig. 1 Particle size distribution of ground and sieved halloysite, Biela Hora

calibration. The instrument was cooled with liquid nitrogen using an LN2 accessory at the set point of −90 °C and flushed with dry nitrogen as a purge gas. The samples were scanned between 0 and 90 °C in the heat–cool–heat cycle with 5 °C min^{-1} rate of temperature change. Melting point was identified as a maximum of the melting endotherm in the first and second heating runs. The value of 139.5 J g^{-1} [19] was used as the heat of melting of 100 % crystalline PCL in calculating its crystallinity. The non-isothermal crystallization kinetics was evaluated empirically by analyzing the cumulative crystallization curves.

Spectrometry

ATR FTIR spectra were recorded on a Nicolet Nexus 870 FTIR spectrometer purged with dry air and equipped with a MCT detector at a resolution of 4 cm^{-1}. Samples were measured on a horizontal micro-ATR Golden Gate unit (SPECAC) with a diamond prism. The spectra were processed by advanced ATR correction using the OMNIC software.

The model quantum chemical calculations were performed at the density functional level of theory (DFT) using the Gaussian 09 program package [20]. The B3LYP functional and the 6-311 + G(2d,p) basis set were used and the optimizations were unconstrained. Vibrational frequencies of the normal modes were scaled by the standard scaling factor 0.9692 [21].

Characterization of structure

The structure of PCL spherulites was examined using polarized light microscope Zetopan. The thin-layer (∼50 μm) samples were observed.

The fracture surface of composites was examined using scanning electron microscope (SEM) Tesla BS-300 SEM. Prior to analysis, the fracture surfaces were sputter-coated with a gold layer of 40–50 nm thickness using a Balzers SCD050 coating machine.

Results and discussion

Effect of urea modification on thermal stability of HNT

Particle size distribution of ground and sieved halloysite from Biela Hora, Slovakia, is obvious from Fig. 1. The dimensions of halloysite nanotubes are shown in Fig. 2. More detailed characterization of HNT applied is described elsewhere [18].

The TG-DTG patterns of the halloysite and the halloysite-urea complex are given in Fig. 3a and b, respectively.

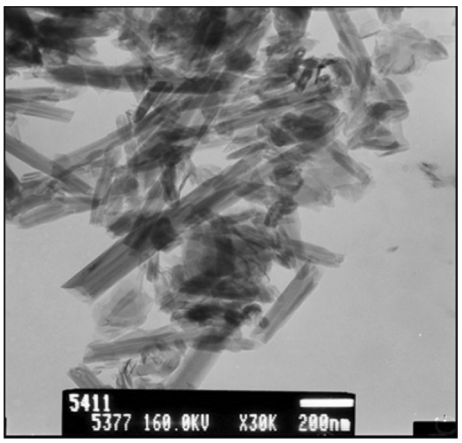

Fig. 2 TEM image of halloysite nanotubes

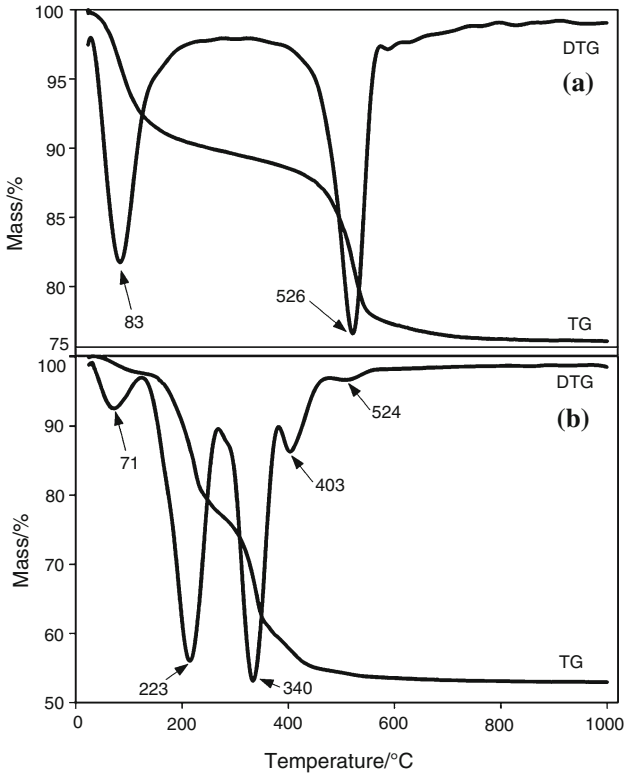

Fig. 3 TG-DTG patterns of **a** halloysite and **b** halloysite-urea complex

The neat halloysite contains 10.5 % water which is lost at 83 °C at maximum rate. Dehydroxylation of the mineral occurs at 526 °C with a mass loss of 14.0 % which is close to the theoretical value.

The complex contains 2.6 % adsorbed water. Intercalated and surface-adsorbed urea decomposes at 233 and 340 °C (through the formation of biuret). The total amount of the reagent lost is 57.4 %. The dehydroxylation of the thermally deintercalated mineral takes place at 403 °C. The

small mass loss step at 524 °C belongs to the dehydroxylation of the non-expanded mineral [22].

Mechanical properties of PCL

From Table 1, it is evident that addition of 5 mass% of unmodified halloysite leads to improvement of tensile strength and Young modulus when compared to the neat PCL. Our results, however, do not correspond to much more significant improvement of PCL mechanical properties observed in recently published paper [17]. These differences are connected primarily with diverse way and conditions of composite preparation, but also with diverse structure parameters and aspect ratio of used halloysite types as well as formation of halloysite agglomerates in the PCL matrix (Fig. 4a).

Unlike unmodified halloysite-based PCL composites, remarkable improvement of elongation (nearly 50 % over composite with unmodified HNT) and Young modulus was observed in composites based on the urea-modified halloyisite. As it is evident from Fig. 4 (similarly to our earlier results on PP/HNT composites [18]), urea modification significantly improved the dispersion of HNT and homogeneity of PCL composites (Fig. 4b). We ascribe this improvement to change of interfacial energy between HNT-urea and PCL [23].

To highlight the effect of urea itself, we further studied the role of urea on PCL properties. By adding just 1 mass% of urea, the improvement of mechanical properties, especially of maximum stress, was comparable to that of the PCL composite containing 5 mass% of untreated halloysite (Table 1).

As shown below (Table 2), urea has a negligible effect on PCL crystallinity evaluated by DSC. Therefore, improved mechanical properties are most probably caused by PCL/urea interactions, i.e., an H-bond-based physical network (interchain H-bond linkage) as indicated by FTIR discussed in the next chapter. As a result, urea has a multiple effect in the PCL/HNT system (influencing the matrix parameters and HNT dispersion).

FTIR characterization of urea-induced interactions

ATR FTIR spectra of neat PCL and the mixtures of PCL with 1 and 2 % of urea are shown in Fig. 5. The band at 1,726 cm^{-1} is assigned to the C=O stretching vibration of crystalline PCL, while the band at 1,677 cm^{-1} corresponds to the C=O stretching mode of pure urea. Significant spectral changes are detected in the spectra of mixtures compared to neat PCL, which suggests strong interactions with urea. New relevant bands appear at 1,737; 1,693; and 1,655 cm^{-1}. The band at 1,737 cm^{-1}, which can also be

Table 1 Effect of additives on mechanical properties of PCL

Sample composition	Max stress/MPa	Strain at break/%	Yield stress/MPa	Modulus/MPa
Neat PCL	28.4	816	16.6	238
PCL + 0.2 mass% urea	28.6	829	16.4	242
PCL + 0.5 mass% urea	29.1	845	16	248
PCL + 1.0 mass% urea	31.9	965	15.5	266
PCL + 2.0 mass% urea	30.7	886	15.6	260
PCL + 5 mass% HNT	29.5	589	17.1	258
PCL + 5 mass% urea mod. HNT	33.3	1,100	15.5	297

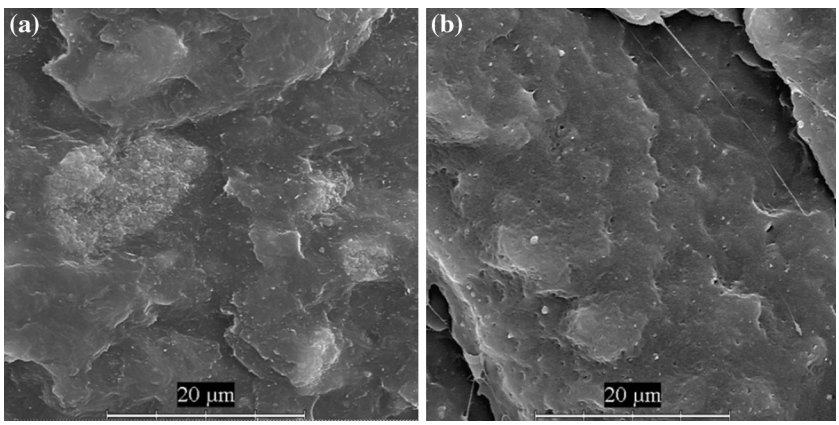

Fig. 4 SEM of fracture surface of **a** PCL/HNT, **b** PCL/(HNT-urea) composites

Table 2 DSC runs and non-isothermal crystallization kinetics

Sample	1st run		2nd run		NIC kinetics		
	T_m/°C	*Cr*/%	T_m/°C	*Cr*/%	RC_i/%	T_i/°C	$\lvert s_i \rvert$/K^{-1}
PCL	61.8	49.1	59.3	39.1	43.5	34.8	23.9
PCL/HNT	62.0	43.8	59.6	40.4	40.0	35.5	26.8
PCL/urea	62.7	48.0	59.1	40.0	44.0	35.7	22.9
PCL/urea-HNT	62.3	48.5	58.9	38.0	43.8	35.8	23.7

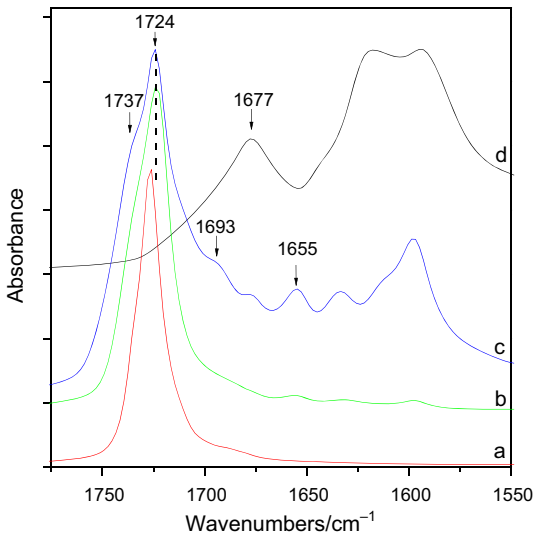

Fig. 5 FTIR spectra of *a* PCL, *b* PCL/urea (1 %), *c* PCL/urea (2 %), *d* urea

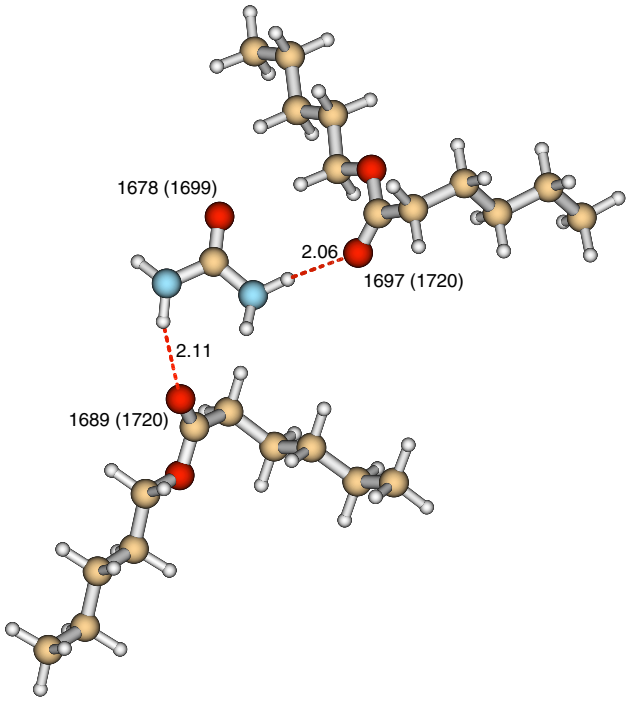

Fig. 6 DFT structure of the hydrogen-bonded complex of two PCL segments and one molecule of urea

detected as a small shoulder in the spectrum of neat PCL, is attributed to the carbonyl groups of the amorphous portion of PCL [24]. The bands at 1,693 and 1,655 cm^{-1} can be assigned to the C=O stretching modes of PCL and urea in the PCL/urea complex that are shifted to lower wavenumbers relative to neat species due to hydrogen bonding interactions.

Proposed interpretation of the FTIR spectra is supported by the results of DFT calculations (Fig. 6). In the model calculations of the PCL—urea interactions, the PCL chains are represented by appropriate chain segments. The optimized structure shown in Fig. 6 demonstrates that two PCL chains can be bound through strong hydrogen bonds of C=O groups with the NH_2 groups of urea. Interaction energy calculated as the difference between the pure electronic energies of the final complex and isolated species is 47.9 kJ mol^{-1}. For the model structure shown in Fig. 6, the calculated frequencies of the C=O stretching vibrations of PCL in the complex are shifted to lower wavenumbers by 23 and 31 cm^{-1} relative to the non-bonded segments. In the case of urea, the C=O stretching vibration in the complex is compared with corresponding value obtained for the hydrogen-bonded urea dimer, which may represent typical conditions in pure urea. In the complex, the frequency of the C=O stretching mode of urea is shifted to lower wavenumbers by 21 cm^{-1}. The DFT calculations do not reproduce the experimental vibrational frequencies exactly; however, the relative values of calculated frequencies are reliable and can be used for the interpretation of the observed frequency shifts.

The DFT-optimized structure of the hydrogen-bonded complex of two PCL segments and one molecule of urea was calculated by the B3LYP/6-311 + G(2d,p) method. Bond lengths are given in Å, and vibrational frequencies (in cm^{-1}) of the C=O stretching modes calculated for the complex are compared (in parenthesis) with corresponding values obtained for the free segment (PCL) and urea dimer.

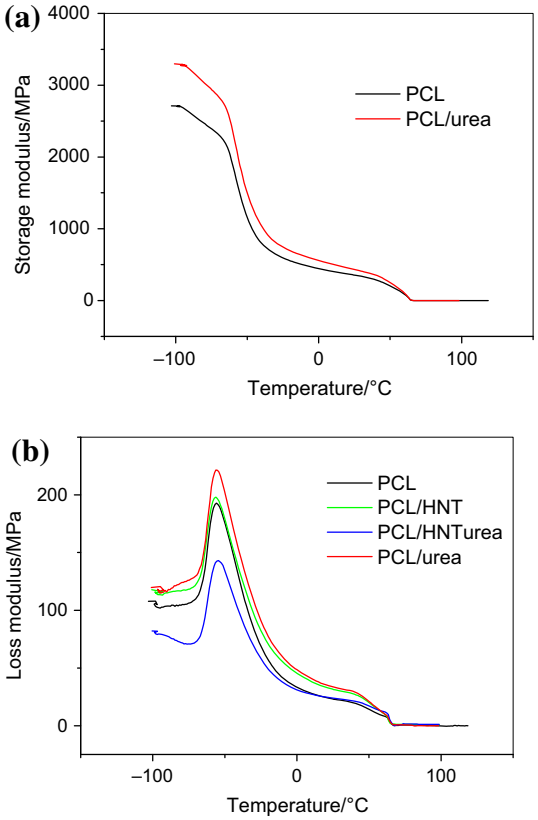

Fig. 7 Temperature dependence of **a** storage and **b** loss moduli

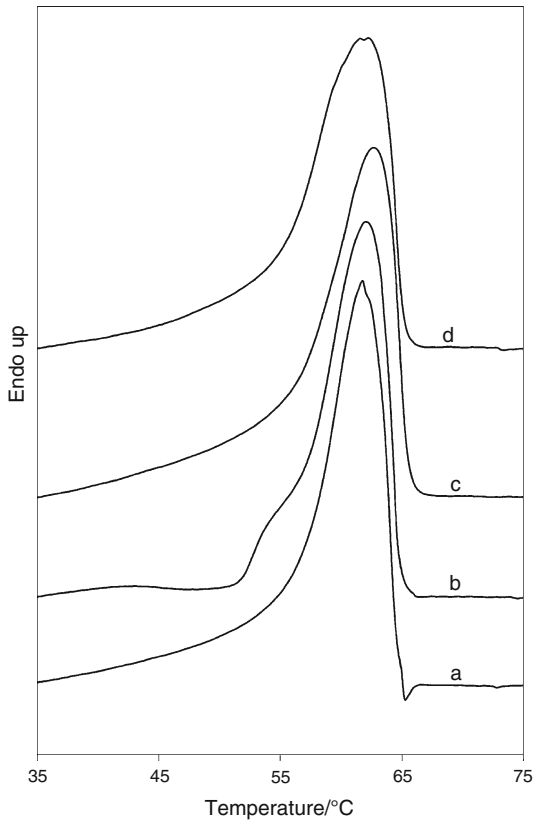

Fig. 8 DSC curves of first heating run: *a* PCL, *b* PCL/HNT, *c* PCL/urea, *d* PCL/urea-HNT

The analogous analysis of composite indicates that HNT–urea interactions could not be detected by ATR FTIR.

Dynamic mechanical analysis

The above fact that improvement of mechanical properties of urea-modified PCL consists predominantly in hydrogen bonding interactions is confirmed by the course of temperature dependence of both storage and loss moduli (Fig. 7). This indicates low thermal stability of interactions obvious from comparable strong decrease in mechanical parameters above the melting points of PCL and urea-modified PCL. DMA further indicates negligible decrease in glass transition temperature (T_g) of PCL due to the presence of urea. The negligible change in T_g by addition of HNT is probably a result of compensation of two effects—usual increase in T_g by added nanofillers, as frequently mentioned in the literature, and higher chain mobility due to increased free volume in the case of anisotropic nanofillers with length far exceeding the typical gyration radii of polymer chains [25, 26]. Presence of urea-modified HNT also leads to slight increase in T_g, which may indicate some urea-mediated hydrogen bond linking between PCL and HNT.

Differential scanning calorimetry

Results of the DSC analysis are summarized in Figs. 8–11 and Table 1. From Table 1, it is obvious that the melting temperatures T_m do not show any significant difference between respective samples, either in the first (Fig. 8) or in the second (Fig. 9) heating run. The melting temperatures T_m are somewhat higher in the first heating run than in the second one. The crystallinities Cr (based on the value 139.5 J g^{-1} for the 100 % crystalline PCL) of all samples are significantly higher in the first run. The results suggest that more perfect PCL crystals, as documented by higher melting temperatures and higher crystallinities, have developed in the as-prepared samples than in the remelted ones.

The non-isothermal crystallization (NIC) kinetics was evaluated purely empirically based on analysis of the cumulative crystallization (CC) curves (Fig. 11). Position of a CC curve on the T-axis relatively to that of neat polymer reflects nucleation effect of added components. The slope of linear part of the CC curves provides information about overall rate of crystallization. Quantitative evaluation of the NIC kinetics in based on two parameters, viz temperature of the inflection point of the CC curve (T_i) and slope of the tangent in the inflection point (s_i). This

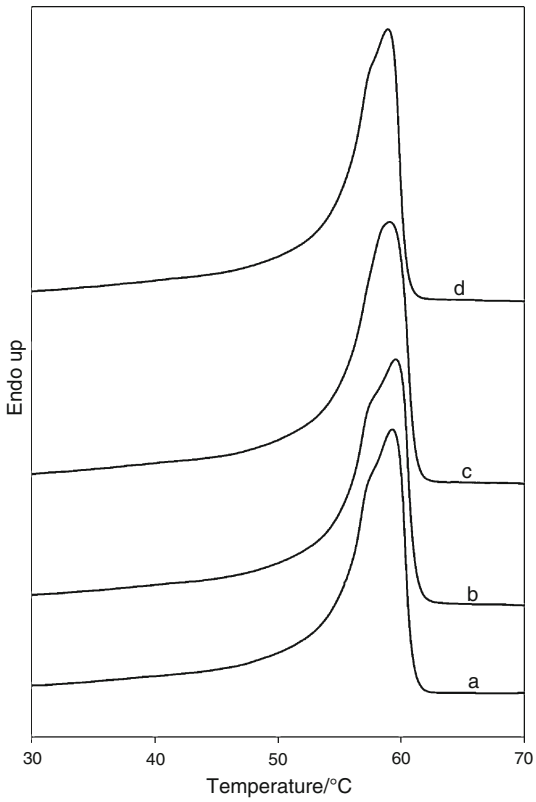

Fig. 9 DSC curves of second heating run: *a* PCL, *b* PCL/HNT, *c* PCL/urea, *d* PCL/urea-HNT

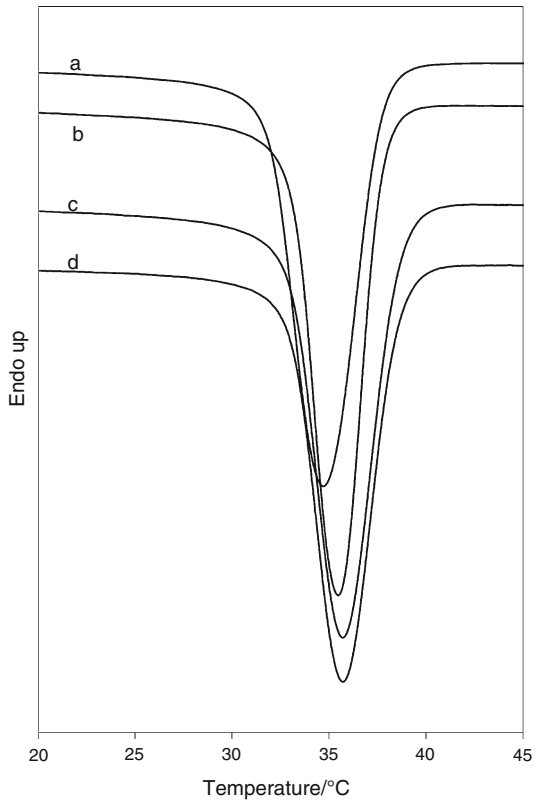

Fig. 10 DSC curves of cooling run: *a* PCL, *b* PCL/HNT, *c* PCL/urea, *d* PCL/urea-HNT

approach has several advantages. It is simple and unambiguous (unlike some theoretical models evaluating early stages of crystallization); it does not refer to any particular crystallization model; its result is the variable directly proportional to the overall rate of crystallization in its maximum and at relatively advanced stage of the crystallization process—see the values of relative crystallinities (RC_i) in Table 1. On the other hand, this approach does not provide information about dimensionality of the crystal growth. To the best of our knowledge, such a simple approach has not yet been reported in the literature.

The parameters obtained in evaluating the NIC kinetics are shown in Table 1. Relative crystallinity RC_i at the point of the kinetic evaluation is 40–45 %. Temperature at the inflection point of the CC curves T_i shifts to higher values for the samples with additives. The addition of urea increases T_i by about 1 °C. The addition of urea-modified HNT has similar affect. The influence of non-modified HNT is lower. Altogether, the effect of additives on the crystallization temperature of PCL is relatively small, which is also apparent from the position of the crystallization exotherms (Fig. 10) and the CC curves (Fig. 11).

The influence of additives on the overall rate of crystallization, as given by the absolute value of the slope of tangent in the inflection point of the CC curves $|s_i|$, is more

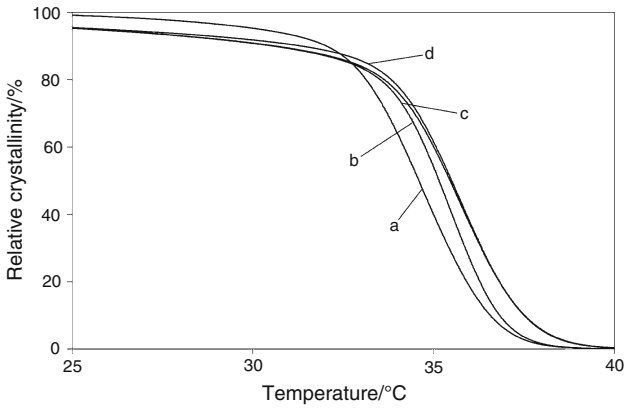

Fig. 11 Cumulative crystallization curves: *a* PCL, *b* PCL/HNT, *c* PCL/urea, *d* PCL/urea-HNT

pronounced. The addition of HNT significantly increases the crystallization rate possibly due to the above-mentioned increase in the free volume and, hence, in the chain mobility. On the other hand, the crystallization rate is reduced by the addition of urea. Here, the chain mobility and thus crystallization rate is probably reduced by the H-bond interactions of urea with PCL—see the FTIR results. In the sample containing urea-modified HNT, these two contradictory effects basically compensate each other.

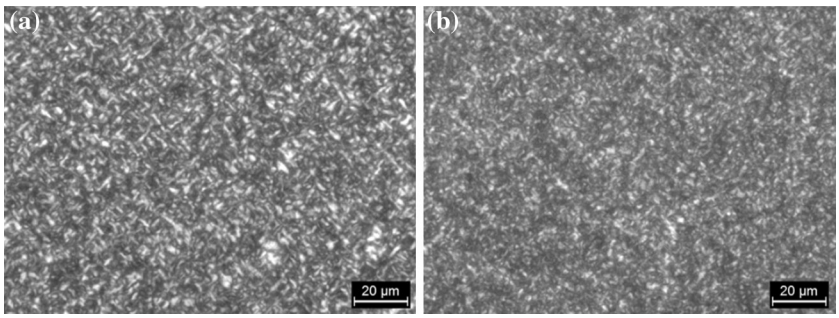

Fig. 12 Polarized light microscopy images of thin-layer samples: **a** PCL, **b** PCL/urea (1 %)

Finally, polarized light microscopy observations (Fig. 12) indicate slightly reduced size of crystalline domains in both PCL/HNT and PCL/urea, when compared with neat PCL.

Conclusions

The results obtained highlight ability of low content ($\leq$1 mass%) of urea to improve mechanical properties of PCL by interchain hydrogen bond linkages as confirmed by FTIR and DMA. The urea modification of HNT using dry grinding technique leads to improved mechanical behavior of the PCL matrix nanocomposites as well. In this case, the matrix modification is accompanied by supporting the dispersion of HNT in the PCL matrix.

The urea and halloysite do not have any marked effect on PCL crystal perfection. The non-isothermal crystallization kinetics, as evaluated by a new purely empirical approach, has revealed moderate nucleating effect if the additives. The addition of HNT significantly increases the overall rate of crystallization, possibly due to increased free volume. Added urea reduces the crystallization rate probably due to H-bond interactions with PCL.

The application urea-modified HNT as well as urea alone presents an original and effective approach of improving PCL end-use properties.

Acknowledgements This work was supported by the Czech Science Foundation (Grant No 13-15255S) and Slovak Scientific Grant Agency (VEGA) Grant No. 1/0361/14. The support of the TÁMOP-4.1.1.C-12/1/KONV-2012-0017 project in the nanocomplex preparation is also gratefully acknowledged.

References

1. Woodruff MA, Hutmacher DW. The return of a forgotten polymer: polycaprolactone in the 21st century. Prog Polym Sci. 2010;35:1217–56.
2. Labet M, Thielemans W. Synthesis of polycaprolactone: a review. Chem Soc Rev. 2009;38:3484–504.
3. Wu D, Zhang Y, Yuan L, Zhang M, Zhou W. Viscoelastic interfacial properties of compatibilized poly (ε-caprolactone)/polylactide blend. J Polym Sci B Polym Phys. 2010;48:756–65.
4. Maglio G, Migliozzi A, Palumbo R, Immirzi B, Volpe MG. Compatibilized poly(ε-caprolactone)/poly(L-lactide) blends for biomedical uses. Macromol Rapid Commun. 1999;20:236–8.
5. Choi N-S, Kim C-H, Cho KY, Park J-K. Morphology and hydrolysis of PCL/PLLA blends compatibilized with P(LLA-co-CL) or P(LLA-b-CL). J Appl Polym Sci. 1992;86:1892–8.
6. Rao RU, Suman KNS, Rao VK, Bhanukiran K. Study of rheological and mechanical properties of biodegradable polylactide and polycaprolactone blends. Int J Eng Sci Technol. 2011;3:6259–65.
7. Chen Q-H, Li X-F, Lin J-H. Preparation and properties of biodegradable bamboo powder/polycaprolactone composites. J For Res. 2009;20:271–4.
8. Neppalli R, Marega C, Marigo A, Bajgai MP, Kim HY, Causin V. Improvement of tensile properties and tuning of the biodegradation behavior of polycaprolactone by addition of electrospun fibers. Polymer. 2011;52:4054–60.
9. Fukushima K, Tabuani D, Camino G. Nanocomposites of PLA and PCL based on montmorillonite and sepiolite. Mater Sci Eng C. 2009;29:1433–41.
10. Chen B, Evans JRG. Poly(ε-caprolactone)-clay nanocomposites: structure and mechanical properties. Macromolecules. 2006;39:747–54.
11. Ludueña LN, Vázquez A, Alvarez VA. Effect of the type of clay organo-modifier on the morphology, thermal/mechanical/impact/barrier properties and biodegradation in soil of polycaprolactone/clay nanocomposites. J Appl Poly Sci. 2013;128:2648–57.
12. Istrate OM, Chen B. Porous exfoliated poly(ε-caprolactone)/clay anocomposites: preparation, structure, and properties. J Appl Polym Sci. 2012;125:102–12.
13. Di Maio E, Iannace S, Sorentia L, Nicolais L. Isothermal crystallization in PCL/clay nanocomposites investigated with thermal and rheometric methods. Polymer. 2004;45:8893–900.
14. Alateyah AI, Dhakal HN, Zhang ZY. Processing, properties, and applications of polymer nanocomposites based on layer silicates: a review. Adv Polym Technol. 2013. doi:10.1002/adv.21368.
15. Du M, Guo B, Jia D. Newly emerging applications of halloysite nanotubes: a review. Polym Int. 2010;59:574–82.
16. Handge UA, Hedicke-Höchstötter K, Altstädt V. Composites of polyamide 6 and silicate nanotubes of the mineral halloysite: influence of molecular weight on thermal, mechanical and rheological properties. Polymer. 2010;51:2690–9.
17. Lee K-S, Chang Y-W. Thermal, mechanical, and rheological properties of poly(ε-caprolactone)/halloysite nanotube nanocomposites. J Appl Polym Sci. 2013;128:2807–16.
18. Khunova V, Kristof J, Kelnar I, Dybal J. The effect of halloysite modification combined with in situ matrix modifications on the structure and properties of polypropylene/halloysite nanocomposites. Express Polym Lett. 2013;7:471–9.
19. Guo Q, Groeninckx G. Crystallization kinetics of poly(ε-caprolactone) in miscible thermosetting polymer blends of epoxy resin and poly(ε-caprolactone). Polymer. 2001;42:8647–55.

20. Frisch MJ, Trucks GW, Schlegel HB, Scuseria GE, Robb MA, Cheeseman JR, Scalmani G, Barone V, Mennucci B, Petersson GA, Nakatsuji H, Caricato M, Li X, Hratchian HP, Izmaylov AF, Bloino J, Zheng G, Sonnenberg JL, Hada M, Ehara M, Toyota K, Fukuda R, Hasegawa J, Ishida M, Nakajima T, Honda Y, Kitao O, Nakai H, Vreven T, Montgomery JA Jr, Peralta JE, Ogliaro F, Bearpark M, Heyd JJ, Brothers E, Kudin KN, Staroverov VN, Kobayashi R, Normand J, Raghavachari K, Rendell A, Burant JC, Iyengar SS, Tomasi J, Cossi M, Rega N, Millam JM, Klene M, Knox JE, Cross JB, Bakken V, Adamo C, Jaramillo J, Gomperts R, Stratmann RE, Yazyev O, Austin AJ, Cammi R, Pomelli C, Ochterski JW, Martin RL, Morokuma K, Zakrzewski VG, Voth GA, Salvador P, Dannenberg JJ, Dapprich S, Daniels AD, Farkas Ö, Foresman JB, Ortiz JV, Cioslowski J, Fox DJ. Gaussian 09, Revision C.01. Wallingford, CT: Gaussian Inc.; 2010.
21. Merrick JP, Moran D, Radom L. An evaluation of harmonic vibrational frequency scale factors. J Phys Chem A. 2007;111: 11683–700.
22. Horváth E, Kristóf J, Kurdi R, Makó É, Khunová V. Study of urea intercalation into halloysite by thermoanalytical and spectroscopic techniques. J Therm Anal Calorim. 2011;105:53–9.
23. Sumita M, Sakata K, Asai S, Miyasaka K, Nakagawa H. Dispersion of fillers and the electrical conductivity of polymer blends filled with carbon black. Polym Bull. 1991;25:265–71.
24. Wang J, Cheung MK, Mi Y. Miscibility and morphology in crystalline/amorphous blends of poly(caprolactone)/poly(4-vinylphenol) as studied by DSC, FTIR, and solid state NMR. Polymer. 2002;43:1357–64.
25. Cai N, Dai Q, Wang Z, Luo X, Xue Y, Yu F. Toughening of electrospun poly(L-lactic acid) nanofiber scaffolds with unidirectionally aligned halloysite nanotubes. J Mater Sci. 2014;. doi:10.1007/s10853-014-8703-4.
26. Liu M, Guo B, Du M, Jia D. Drying induced aggregation of halloysite nanotubes in polyvinyl alcohol/halloysite nanotubes solution and its effect on properties of composite film. Appl Phys A Mater. 2007;88:391–5.